J Neurophysiol 109: 1174–1181, 2013.
First published November 28, 2012; doi:10.1152/jn.01168.2011.

Characterizing the conductance underlying depolarization-induced slow current in cerebellar Purkinje cells

Yu Shin Kim,[1] Eunchai Kang,[2,4] Yuichi Makino,[1] Sungjin Park,[1] Jung Hoon Shin,[1] Hongjun Song,[1,2,3,4] Pierre Launay,[5,6,7] and David J. Linden[1]

[1]*Department of Neuroscience, Johns Hopkins University School of Medicine, Baltimore, Maryland;* [2]*Institute for Cell Engineering, Johns Hopkins University School of Medicine, Baltimore, Maryland;* [3]*Department of Neurology, Johns Hopkins University School of Medicine, Baltimore, Maryland;* [4]*Predoctoral Training Program in Human Genetics, Johns Hopkins University School of Medicine, Baltimore, Maryland;* [5]*Institut National de la Santé et de la Recherche Médicale U699, Paris, France;* [6]*Equipe Avenir, Institut National de la Santé et de la Recherche Médicale, Paris, France; and* [7]*Université Paris 7-Denis Diderot, Faculté de Médecine, Site Xavier Bichat, Paris, France*

Submitted 28 December 2011; accepted in final form 27 November 2012

Kim YS, Kang E, Makino Y, Park S, Shin JH, Song H, Launay P, Linden DJ. Characterizing the conductance underlying depolarization-induced slow current in cerebellar Purkinje cells. *J Neurophysiol* 109: 1174–1181, 2013. First published November 28, 2012; doi:10.1152/jn.01168.2011.—Brief strong depolarization of cerebellar Purkinje cells produces a slow inward cation current [depolarization-induced slow current (DISC)]. Previous work has shown that DISC is triggered by voltage-sensitive Ca influx in the Purkinje cell and is attenuated by blockers of vesicular loading and fusion. Here, we have sought to characterize the ion channel(s) underlying the DISC conductance. While the brief depolarizing steps that triggered DISC were associated with a large Ca transient, the onset of DISC current corresponded only with the Ca transient decay phase. Furthermore, substitution of external Na with the impermeant cation *N*-methyl-D-glucamine produced a complete and reversible block of DISC, suggesting that the DISC conductance was not Ca permeant. Transient receptor potential cation channel, subfamily M, members 4 (TRPM4) and 5 (TRPM5) are nonselective cation channels that are opened by Ca transients but do not flux Ca. They are expressed in Purkinje cells of the posterior cerebellum, where DISC is large, and, in these cells, DISC is strongly attenuated by nonselective blockers of TRPM4/5. However, measurement of DISC currents in Purkinje cells derived from TRPM4 null, TRPM5 null, and double null mice as well as wild-type mice with TRPM4 short hairpin RNA knockdown showed a partial attenuation with 35–46% of current remaining. Thus, while the DISC conductance is Ca triggered, Na permeant, and Ca impermeant, suggesting a role for TRPM4 and TRPM5, these ion channels are not absolutely required for DISC.

TRPM4; TRPM5; cation current; calcium

BRIEF STRONG DEPOLARIZATION of cerebellar Purkinje cells, produced either through voltage-clamp commands or burst-activation of excitatory glutamatergic climbing fiber synapses, gives rise to a biphasic inward current. The early component of this inward current is mediated, at least in part, by a Ca-dependent Cl conductance triggered by Ca influx through voltage-sensitive Ca channels (Llano et al. 1991; Shin et al. 2008). We have described an unusually slow component of this inward current (time to peak: 2.0–3.0 s; 90–10% decay time: ~2.8 s), which we have named DISC (for depolarization-induced slow current; Shin et al. 2008; Crepel et al. 2011). DISC is triggered by Ca influx through voltage-gated channels, being blocked by either a cocktail of Ca channel blockers or external Cd ions, and is strongly attenuated by internal application of either an inhibitor of vesicular neurotransmitter transporters (bafilomycin A) or vesicular membrane fusion (botulinum toxin D; Shin et al. 2008), suggesting autocrine action of a neurotransmitter released following Ca influx.

Here, we have sought to identify the current or currents underlying DISC. Our attention turned to the TRP superfamily of ion channels and in particular to transient receptor potential cation channel, subfamily M, members 4 and 5 (TRPM4 and TRPM5), which are the only members that are directly gated by internal Ca concentration. TRPM4 is a nonselective cation channel that conducts Na and K but not Ca (Launay et al. 2002). It is activated by internal Ca (Launay et al. 2004), and its sensitivity to Ca is strongly modulated by phosphatidylinositol-4,5-bisphosphate (Nilius et al. 2006) and protein kinase C (PKC; Earley et al. 2007). TRPM4 is expressed in a wide variety of tissues including heart, lung, skeletal muscle, intestine, prostate, kidney, and liver (Launay et al. 2002; Fonfria et al. 2006).

TRPM5 is ~45% homologous to TRPM4 and shares many of the same channel properties (Hofmann et al. 2003; Ullrich et al. 2005). Like TRPM4, it is activated by internal Ca and fluxes Na and K but not Ca. TRPM5 is expressed in taste cells, where it appears to be necessary for bitter, sweet, and umami taste transduction (Zhang et al. 2003; Damak et al. 2006). TRPM4 and TRPM5 have been reported to be expressed sparsely in brain (Launay et al. 2002; Fonfria et al. 2006; Mrejeru et al. 2011). The electrophysiological profiles of TRPM4 and TRPM5 are provocative, having similarity to the nonspecific cation conductance (I_{CAN}) of neurons and muscle cells (Guinamard et al. 2011). However, little is known about their electrophysiological function in neurons.

METHODS

Slice preparation. Cerebellar slices were prepared from juvenile [postnatal day (P)16 to P22] C57BL/6 mice using standard techniques, in accordance with a protocol approved by the Animal Care and Use Committee at the Johns Hopkins University School of Medicine. Sagittal slices of the cerebellar vermis (250 μm thick) were cut with a vibrating slicer (Leica VT 1000S) using a sapphire blade in ice-cold *N*-methyl-D-glucamine (NMDG)-based cutting solution. This solution

Address for reprint requests and other correspondence: D. J. Linden, Dept. of Neuroscience, the Johns Hopkins University School of Medicine, 725 12 N. Wolfe Street, Baltimore, MD 21205 (e-mail: dlinden@jhmi.edu).

contained the following (in mM): 135 NMDG, 1 KCl, 1.5 $MgCl_2$, 0.5 $CaCl_2$, 1.2 KH_2PO_4, 24.2 choline bicarbonate, and 13 glucose, bubbled with 95% O_2-5% CO_2 to yield pH 7.4. Slices were maintained thereafter in artificial cerebrospinal fluid containing the following (in mM): 124 NaCl, 2.5 KCl, 2.5 $CaCl_2$, 1.3 $MgCl_2$, 1 NaH_2PO_4, 26.2 $NaHCO_3$, and 20 glucose at room temperature. They were then placed in a submerged chamber that was perfused at 2 ml/min with artificial cerebrospinal fluid, also at room temperature and bubbled with 95% O_2-5% CO_2 to yield pH 7.4. GABAzine (5 μM) was added to the recording solution to block $GABA_A$ receptors. Slices were visualized on an upright microscope equipped with infrared differential interference contrast or gradient contrast optics using a ×40 water immersion objective.

Electrophysiology. Whole cell patch-clamp recordings were made from Purkinje cells in the cerebellum using conventional techniques. The pipette solution consisted of the following (in mM): 135 Cs-methanesulfonate, 6 CsCl, 2 $MgCl_2$, 0.15 $CaCl_2$, 0.2 EGTA, 10 HEPES, 4 Na_2-ATP, 0.4 Na_3-GTP, pH 7.2–7.3, and osmolarity = 290 mosM. Pipette resistance varied from 1.5 to 2 MΩ. Cells were voltage clamped using a Multiclamp 700A amplifier (Molecular Devices; Sunnyvale, CA). Unless otherwise noted the command potential was −70 mV. Series resistance was <15 MΩ. Recordings of membrane current were filtered at 1 KHz, digitized at 5 kHz, and collected with pClamp 9 software (Molecular Devices). DISC was induced by a test stimulus consisting of five 10-ms-long depolarizing command pulses from −70 to 0 mV, delivered at 10 Hz.

The following agents were added to the recording bath solution: SR95531 (GABAzine) was purchased from Ascent Scientific (Princeton, NJ) and glibenclamide was purchased from Tocris (Ellisville, MO). All other chemicals were from Sigma (St. Louis, MO).

Mice. TRPM4 null mice were obtained from the laboratory of Pierre Launay, and TRPM5 null mice were purchased from The Jackson Laboratory (Bar Harbor, ME). TRPM4 null mice and wild-type littermates were genotyped as previously described (Barbet et al. 2008). TRPM5 null mice and wild-type littermates were genotyped as described in The Jackson Laboratory genotyping protocol database. TRPM4 or TRPM5 null mice were created by breeding TRPM4 or TRPM5 heterozygotes to allow for littermate wild-type controls. TRPM4/5 double null mice were created by breeding TRPM4 homozygous nulls to TRPM5 homozygous nulls to generate double heterozygotes. Double heterozygotes were then mated to nonsibling double heterozygotes to create TRPM4/5 double nulls and wild-type controls.

Analysis. Patch-clamp data were analyzed offline using Clampfit (Molecular Devices), Origin (OriginLab), and Igor Pro (WaveMetrics) software. Group data were expressed as means ± SE. The Mann-Whitney U test was used to determine significance in pairwise statistical comparisons. The DISC charge transfer was measured from a 1-s-long segment centered at the DISC peak. Offline digital processing of traces was used to high-pass filter the traces at 10 Hz to extract the noise envelope, which tracks DISC amplitude and therefore allows for clear separation between the faster inward current (Ca-sensitive Cl current; Llano et al. 1991) and DISC (Shin et al. 2008). The noise SD was calculated from a 1-s-long segment centered at the DISC peak of the digitally high-pass-filtered traces. The Δ noise SD was calculated by subtracting the noise SD in a 1-s-long sample before depolarization (baseline noise SD) from that during DISC sampling period and normalized by baseline noise SD.

Ca imaging. Fluo-5F (0.3 mM; K_d = 2.3 μM) was added to the pipette solution to measure Ca transients using green emitted light, and 0.3 mM Alexa 594 hydrazide, a cytosolic marker, was added to visualize the soma and dendrite using red-emitted light (both from Invitrogen, Carlsbad, CA). To allow for dye diffusion, 15 min elapsed between the onset of whole cell access and the beginning of imaging. To minimize phototoxicity, 0.1 mM Trolox-C was added to artificial cerebrospinal fluid and the power and exposure time of laser illumination were maintained as low as possible. Single photon Ca imaging was performed with a Zeiss Pascal confocal microscope, using the 488-nm line of an argon laser for excitation of Fluo-5F and a 505-nm dichroic mirror and a 505- to 530-nm bandpass filter to detect the emission of green fluorescence. Ca transients were elicited by the same burst protocol used to trigger DISC: five 10-ms-long depolarizing steps to 0 mV, delivered at 10 Hz. Bursts were delivered at 1-min intervals. Alexa 594 hydrazide was excited with the 543-nm line of a He-Ne laser, and the emitted red fluorescence was collected through a 545-nm dichroic mirror and a 560-nm long-pass filter. Fluo-5F images were acquired at 20 Hz in frame-scan mode with a 128 × 33 pixel region of interest. For analysis, foreground pixels were determined by thresholding the image and were spatially averaged to calculate $\Delta F/F_0$ for each frame. Background correction was performed by subtracting the background fluorescence of a region adjacent to the distal dendrite. Ca signal amplitudes were expressed as $(F_t - F_0)/F_0$. The average fluorescence intensity in the baseline period was taken as F_0. Image J (National Institutes of Health) was used to analyze Ca imaging data using a custom macro.

Immunohistochemistry. Animals were anesthetized with ketamine (100 mg/kg) and xylazine (10 mg/kg) and perfused intracardially with 4% paraformaldehyde in 0.1 M sodium phosphate buffer. After the perfusion, brains were removed and maintained in the same paraformaldehyde solution overnight at 4°C and then washed with PBS. The cerebellum was cut into 50-μm slices on a vibrating tissue slicer. For labeling, free-floating slices were incubated with 5% preimmune donkey or goat serum in 0.2% Triton X-100 PBS to block nonspecific antibody reactions. After several rinses with PBS, the slices were incubated overnight with primary antibodies: rabbit anti-human TRPM4 (from the laboratory of Pierre Launay, 1:500) and rabbit anti-rat TRPM5 (from the laboratory of Robert Margolskee, 1:200). After several rinses with PBS, the slices were then incubated with Alexa Fluor 488- or 546-conjugated secondary antibodies to rabbit IgG or guinea pig IgG (Jackson ImmunoResearch) at a dilution of 1:500. The images were acquired using a LSM Pascal laser-scanning confocal microscope (Zeiss) with a ×40 water immersion objective.

Design, production, and validation of engineered short hairpin RNA lentivirus. The targeting sequence of short hairpin (sh)RNA directed against mouse TRPM4 was 5′-CTAACTCACTGATCCGAAA-3′. Scrambled sequence (5′-TTCTCCGAACGTGTCACGT-3′) without homology to any known mRNA was used for the nonsilence control shRNA (Ma et al. 2009). shRNA and EGFP were coexpressed under the control of human U6 and ubiquitin promoters, respectively, in an engineered lentiviral FUGW vector (see Fig. 6*A*; Lois et al. 2002). High titers of engineered lentivirus (1×10^8 U/ml) were produced by cotransfection of the transfer vector FUGW with vesicular stomatitis viral envelope glycoprotein vector (VSVG) and the HIV-1 packaging vector Δ8.9 into HEK293T cells, followed by ultracentrifugation of viral supernatant as previously described (Duan et al. 2007). The pH of the concentrated lentivirus solution was adjusted using NaOH. To validate the efficacy and specificity of shRNA, lentiviruses carrying shRNA against mouse TRPM4 and control were transduced into a mouse adult neural progenitor cell line. These cells were harvested for Western blot 72 h later. Endogenous TRPM4 protein levels were measured in tissue derived from 17-day-old C57BL/6 mice. These samples were isolated in cell lysis buffer [10 mM Tris pH 7.4, 150 mM NaCl, 2 mM EDTA, 1% Triton X-100, 0.1% SDS, and 1 mM vanadate proteinase inhibitor (Roche)]. Protein concentration was determined by the NanoDrop 2000 assay method (Thermo Scientific). Twenty microliters of protein were separated on 12% SDS-PAGE and transferred to a PVDF membrane. The membrane was blocked with TBS (50 mM Tris·HCl and 500 mM NaCl at pH 7.5) containing 0.5% Tween and 3% BSA and was incubated with primary antibody (TRPM4; rabbit, 1:500; laboratory of Pierre Launay) or GAPDH (mouse, 1:2,000; Abcam) overnight at 4°C. It was then washed and incubated with horseradish peroxidase-conjugated secondary antibodies against mouse IgG or rabbit IgG for 1 h at room temperature.

Quantification of the Western blots was performed using FluorChem8900 software.

In vivo stereotaxic injection and transduction with engineered lentivirus. Purkinje cells were transduced by injection of engineered lentiviruses expressing shRNA and EGFP into lobules IX and X of the cerebellar vermis. Young C57BL/6 mice (P17–P19) were anesthetized with an intraperitoneal injection of ketamine (110 mg/kg) and xylazine (10 mg/kg) and placed in a stereotaxic device (Stoelting). The muscles and fascia were retracted to expose the skull overlying the posterior cerebellum. A small opening was then drilled in the skull to expose the dura overlying cerebellar lobules IX and X. The dura was then removed. A glass pipette with 30- to 40-μm-tip diameter was filled with mineral oil and connected to a pressure injection device (Nanojet II, Drummond Scientific). The tip of the glass pipette was then filled with 3–4 μl of lentivirus solution, and injections were made in the cortex of cerebellar lobules IX and X, in the vermis, at a depth of 0.7–1.2 mm. We positioned the pipette at an angle 35° above the horizontal plane. For each injection, the volume of virus-containing solution was 0.8–1 μl that was delivered over a 5-min period. The pipette was then left in place for 5 min before it was withdrawn to reduce backflow. For each mouse, four different sites were injected, two at the midline and two sites on either side of the midline, ~0.5- to 1-mm lateral. Following injection, the mice were group housed under standard conditions. After a delay of 1 wk, the mice (P24–P26 days old) were anesthetized with isoflurane. The cerebellum was then removed, and cerebellar slices were prepared using standard techniques.

RESULTS

To determine if the DISC conductance involves Ca flux, we performed simultaneous confocal Ca imaging and whole cell patch-clamp recording from Purkinje cells in cerebellar slices derived from juvenile mice. Previous work from our group had shown that a brief burst depolarization protocol (consisting of five 10-ms-long step depolarization from −70 to 0 mV at 10 Hz) could reliably induce robust DISC in Purkinje cells of cerebellar lobules IX and X (Kim et al. 2009). Here we have repeated that protocol but have supplemented the pipette solution with the Ca indicator dye Fluo-5F (0.3 mM) and the cytosolic marker dye Alexa Fluor 594 (0.3 mM). Figure 1 shows a representative Purkinje cell in which brief burst depolarization produced DISC that peaked at 2.43 s after burst onset, similar to that previously reported (Shin et al. 2008; Crepel et al. 2011; Kim et al. 2009). The simultaneously recorded Ca transient in the distal dendritic region of this cell revealed a peak $\Delta F/F_0$ of 7.78 that was achieved 0.65 s after burst onset. The decay phase of this Ca transient was well fit by double exponentials with τ_{fast} = 0.66 s and τ_{slow} = 5.48 s. Importantly, at t = 2.53 s, which was the peak of DISC, the Ca transient had decayed to $\Delta F/F_0$ = 1.31.

Population measurements in the distal dendritic compartment revealed a peak $\Delta F/F_0$ of 6.94 ± 1.31 that was achieved at t = 0.73 ± 0.03 s after burst onset (n = 5). The decay phase was well fit with τ_{fast} = 0.61 ± 0.06 s and τ_{slow} = 3.87 ± 0.67. At the peak of DISC, at t = 2.50 ± 0.14 s, Ca transients had decayed to $\Delta F/F_0$ = 1.34 ± 0.12, which is ~19% of the Ca transient peak. In the somatic compartment, the peak $\Delta F/F_0$ was lower and slightly slower: peak $\Delta F/F_0$ of 3.85 ± 1.17 that was achieved at t = 0.91 ± 0.19 s after burst onset (n = 5). The decay phase was well fit with τ_{fast} = 1.02 ± 0.31 s and τ_{slow} = 3.67 ± 0.50 s. In the proximal dendrite, Ca transients were intermediate between the distal dendrite and the soma: peak $\Delta F/F_0$ of 5.41 ± 1.48 that was achieved at t = 0.95 ± 0.24 s after burst onset (n = 5). The decay phase was well fit with τ_{fast} = 0.77 ± 0.12 s and τ_{slow} = 3.97 ± 0.99 s. These findings indicate that, while depolarization-evoked Ca influx is important as a trigger for DISC (Shin et al. 2008), the DISC conductance does not flux substantial amounts of Ca.

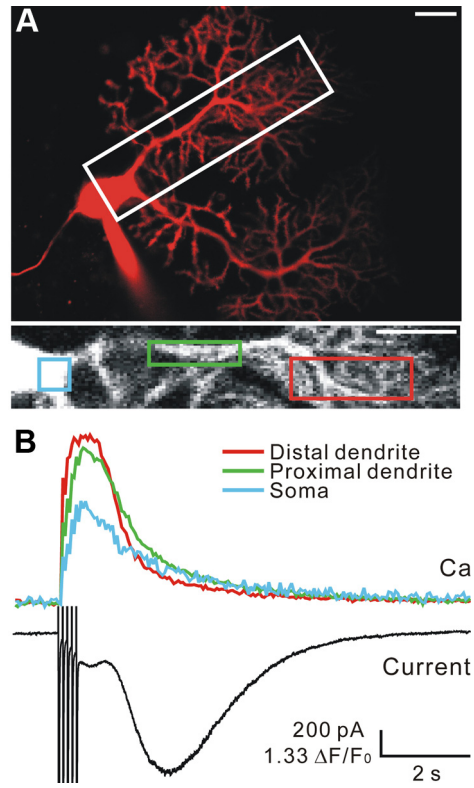

Fig. 1. Depolarization-induced slow current (DISC) expression does not produce significant Ca influx. *A*: simultaneous confocal Ca imaging and whole cell patch-clamp recording were performed using Purkinje cells loaded with both Fluo-5F (0.3 mM), a Ca indicator, and Alexa Fluor 594 hydrazide (0.3 mM), a cytosolic marker. *A*, *top*: projection of z series confocal images of a Purkinje cell filled with Alexa Fluor 594 and the attached patch pipette. *A*, *bottom*: peak Fluo-5F Ca signal in a region of interest indicated by white box at *top*. Blue green and red boxes indicate subregions of interest used for Ca transient measurement in soma, proximal dendrite, and distal dendrite, respectively. Scale bars: 20 μm for both *top* and *bottom*. *B*: single, representative unaveraged Ca transient traces in the 3 subregions and simultaneous DISC current recording. A brief burst depolarization protocol was used that consisted of five 10-ms-long step depolarizations from −70 to 0 mV at 10 Hz. Note that the onset and peak of DISC current correspond to the falling phase of the depolarization-evoked Ca transient. Scale bar: 1.33 $\Delta F/F_0$, 2 s for Ca transient trace and 200 pA, 2 s for current trace. The peak of the distal dendritic Ca transient has a flattened shape. This shape is not the result of dye saturation as other Ca transients recorded in this cell routinely exceeded this peak $\Delta F/F_0$ and displayed a sharper shape (data not shown).

If Ca influx is important in triggering DISC (Shin et al. 2008) but Ca influx does not appear to mediate the DISC conductance (Fig. 1), then what cation(s) do underlie it? Na influx is an obvious candidate. To address this possibility, we recorded baseline DISC responses and then briefly switched from normal external saline [total extracellular Na concentration of ~151 mM] to an external saline in which NaCl was substituted with *N*-methyl-D-glucamine-Cl (NMDG; total extracellular Na concentration of ~27 mM). NMDG is impermeant for most monovalent cation channels such as Ca-blockable monovalent cation channel in the ectoderm of the chick embryo as well as Ca-impermeable AMPA and kainate receptors (Sabovcik et al. 1995; Burnashev et al. 1996). This

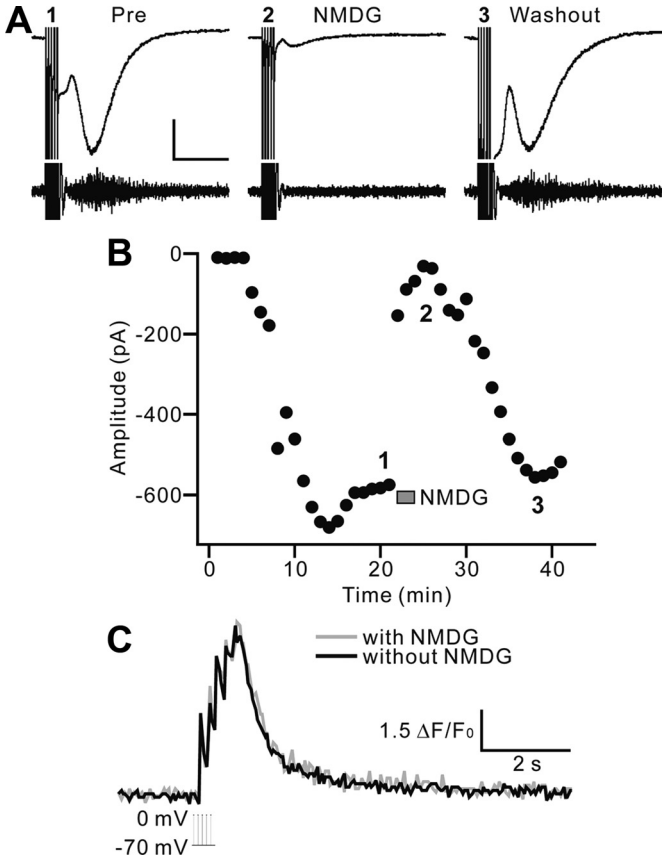

Fig. 2. DISC is reversibly abolished by replacing external Na with *N*-methyl-D-glucamine (NMDG). *A*: baseline DISC was recorded in normal external saline and then briefly switched to an external saline in which NaCl was substituted with NMDG, an impermeant molecule for most monovalent cation channels. Then, the NMDG-containing saline was washed out with normal external saline. Representative single, unaveraged DISC current and filtered noise envelope traces are shown. The noise envelope, which tracks DISC amplitude, allows for clear separation between the faster inward current (Ca-sensitive Cl current; Llano et al. 1991) and DISC (Shin et al. 2008). Scale bar: 200 pA, 2 s for DISC current trace and 29.1 pA, 2 s for noise envelope. Attenuation of the fast inward current by Na replacement with NMDG, as seen in these traces, was a variable and inconsistent phenomenon. *B*: DISC current amplitude was plotted as a function of time to show the complete, transient blockade of DISC by NMDG-substituted external saline in a single representative cell from a group of 7. *C*: representative single, unaveraged depolarization-evoked Ca responses for a representative Purkinje cell in normal (without NMDG, black trace) and NMDG-substituted (gray trace) external saline.

treatment produced a near-complete blockade of DISC that could be recovered upon washout (Fig. 2). The population measures showed that DISC charge transfer was reduced to 9 ± 3% of baseline by Na substitution with NMDG (n = 7 cells). When depolarizing burst-evoked Ca transients were measured in a separate set of cells, NMDG substitution caused a modest increase in the amplitude of the evoked Ca transient (Fig. 2*C*; 116 ± 7% of baseline, n = 5), possibly as a result of attenuating extracellular Na/intracellular Ca exchange. In any case, this observation suggests that the blockade of DISC by Na substitution with NMDG is not secondary to a block of depolarization-evoked Ca influx.

The DISC conductance is triggered by Ca but appears to involve Na influx but not significant Ca influx. It is likely that K efflux also occurs but that was not specifically tested here. This weakly Ca-permeable cation current matches the properties of the TRPM4 conductance studied in various cell types and locations, as well as heterologous expression systems (Launay et al. 2002; Vennekens and Nilius 2007). It also closely matches the properties of the TRPM5 conductance (Hofmann et al. 2003; Guinamard and Simard 2011). As such, we wished to determine if TRPM4 and TRPM5 proteins are expressed in those cerebellar Purkinje cells where robust DISC can be recorded. To this end, we performed floating section immunohistochemistry using a polyclonal antiserum directed against a 17 amino acid peptide from human TRPM4 and a 22 amino acid peptide from mouse TRPM5 (Fig. 3). Sections of juvenile mouse cerebellum showed clear immunoreactivity for both TRPM4 and TRPM5 in the soma and dendrites of Purkinje cells from lobule IX, where robust DISC is routinely recorded and much lower levels in lobule VI where DISC is weak (Kim et al. 2009). For TRPM4 staining, mean pixel intensity for the Purkinje cell layer was 134.23 ± 7.06 in lobule IX and 45.47 ± 0.44 in lobule VI (arbitrary units, n = 4). For TRPM5 staining, mean pixel intensity for the Purkinje cell layer was 119.69 ± 15.20 (n = 4) in lobule IX and 32.75 ± 1.53 in lobule VI. In the cerebellar molecular layer, which contains the Purkinje cell dendrites, TRPM4 staining yielded a mean pixel intensity of 76.70 ± 4.82 in lobule IX and 44.28 ± 0.55 in lobule VI. For TRPM5 staining, mean pixel intensity for the molecular layer was 82.80 ± 10.47 (n = 4) in lobule IX and 29.84 ± 1.44 in lobule VI. The specificity of these antibodies was conformed by experiments in which TRPM4 and TRPM5 antibodies were applied to tissue from their corresponding null mice, yielding only background levels of immunoreactivity (Fig. 3). Controls with no primary antibody also showed background levels of immunoreactivity.

As a first test of the hypothesis that TRPM4 and/or TRPM5 underlie the DISC conductance, we used a series of TRPM4 and TRPM5 blocking drugs: glibenclamide (100 μM), flufenamic acid (100 μM), and 9-phenanthrol (100 μM; Fig. 4). A control group, which was simply recorded for 20 min after stable DISC was achieved, showed a mean DISC charge transfer amplitude of 0.61 ± 0.02 nC (n = 5). All three of these drugs produced strong attenuation of DISC charge transfer (Fig. 4). The mean DISC charge transfer after application of glibenclamide was 0.13 ± 0.06 nC, which was 22 ± 10% of predrug baseline (n = 5; $P < 0.01$, compared with control). For flufenamic acid it was 0.04 ± 0.01 nC and 6 ± 2% of predrug baseline (n = 5; $P < 0.01$), and for 9-phenanthrol it was 0.06 ± 0.01 nC and 10 ± 3% (n = 5; $P < 0.01$). While these drugs have been used to block TRPM4 or TRPM5 in heterologous expression systems (Ullrich et al. 2005; Grand et al. 2008) or various cardiac cells including sinoatrial node cells and ventricular cardiomyocytes (Guinamard et al. 2006; Demion et al. 2007), they also have nonspecific effects on other ion channels and transporters. Glibenclamide affects the cystic fibrosis transmembrane conductance regulator Cl channels, other Cl channels, and ATP-sensitive K channels (Ashcroft and Gribble 1999; Pompermayer et al. 2007). Flufenamic acid has side-effects on Ca-activated current, K channels, and other currents (Takahira et al. 2005; Gardam et al. 2008). 9-Phenanthrol, which has been reported to block TRPM4 but not TRPM5 (Grand et al. 2008), also blocks the cystic fibrosis transmembrane conductance regulator and other ATP-binding cassette proteins.

Because of the lack of specific blockers of TRPM4 and TRPM5, we turned to previously characterized null mice

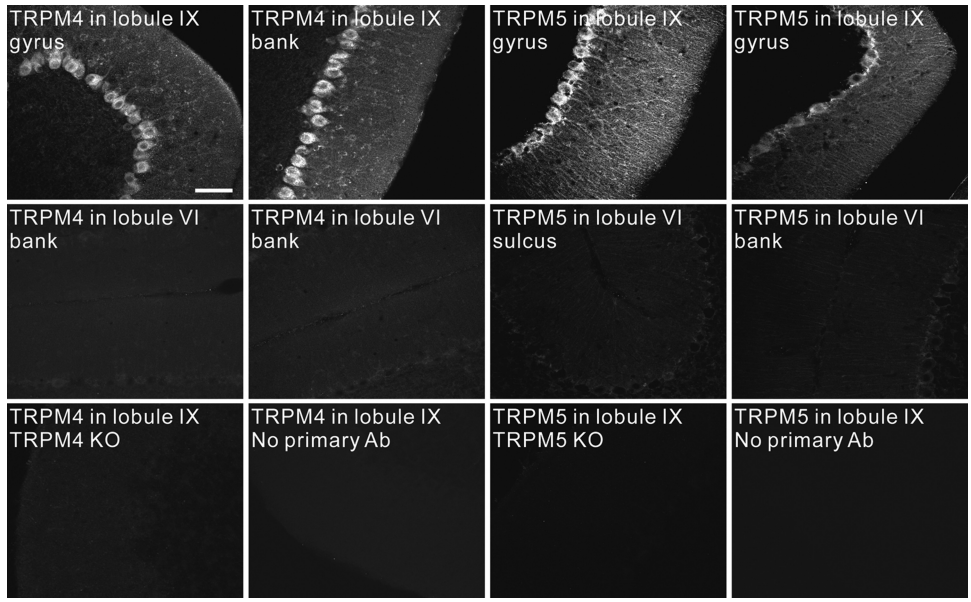

Fig. 3. Transient receptor potential cation channel, subfamily M, member 4 (TRPM4) and TRPM5 are strongly expressed in Purkinje cells of those posterior cerebellar regions where DISC is largest. Representative confocal images from different subregions of the cerebellum are shown. Immunohistochemistry using polyclonal antibodies directed against the human TRPM4 and the mouse TRPM5 proteins was performed using free-floating sagittal slices of cerebellar vermis. Strong immunoreactivity for TRPM4 and TRPM5 proteins was seen in the soma, primary, and secondary dendrites of Purkinje cells located in lobule IX, where robust DISC is routinely recorded (*top*). By contrast, very weak immunoreactivity for both ion channels was seen in Purkinje cells in the more anterior lobule VI, where DISC is typically small (*middle*). *Bottom*: controls with either antibodies applied to the corresponding null mouse (*left*) or without primary antibody (*right*). Scale bar: 50 μm. KO, knockout.

(TRPM4: Barbet et al. 2008; TRMP5: Riera et al. 2009), singly and also crossed to produce double nulls. Because the genetic background of each of these 3 mutant mice is different, each must be compared with its own wild-type littermate (Fig. 5). Purkinje cells in brain slices derived from TRPM4 null mice showed DISC charge transfer that was 46 ± 7% of that in age-matched wild-type littermates (TRPM4 KO: 0.27 ± 0.06 nC, $n = 40$; WT control: 0.60 ± 0.07 nC, $n = 31$; $P < 0.001$). By contrast, DISC in TRPM5 nulls was not significantly attenuated at 80 ± 15% of control (TRPM5 KO: 0.49 ± 0.06 nC, $n = 19$; WT control: 0.62 ± 0.08, $n = 15$). Finally, Purkinje cells from TRPM4/5 double null mice expressed DISC at levels 35 ± 9% of their age-matched wild-type littermates. (TRPM4/5 DKO: 0.23 ± 0.04 nC, $n = 28$; WT control: 0.64 ± 0.04 nC, $n = 46$; $P < 0.001$).

Might the attenuated DISC in TRPM4 KO and TRPM4/5 DKO Purkinje cells be a consequence of attenuated voltage-evoked Ca transients? To address this possibility, we performed Ca imaging experiments in conjunction with DISC-inducing depolarizing stimulation. Measurements in distal dendritic compartments revealed no significant difference in either peak or integrated Ca signals when compared with C57BL/6 WT controls. The peak Ca transients were $\Delta F/F_0 = 6.94 \pm 1.31$ in WT ($n = 5$; these are the same cells as shown in Fig. 1 and described in the accompanying text), 6.66 ± 1.11 in TRPM4 KO ($n = 5$), and 5.75 ± 0.97 in TRPM4/5 DKO ($n = 5$). In addition, no significant differences emerged when somatic or proximal dendritic regions of interest were measured (Fig. 6*C*).

We next considered the possibility that the reason that DISC was only partially attenuated in the TRPM4 null Purkinje cells (Fig. 5) was a result of some form of compensation in this mutant mouse: perhaps knockout of TRPM4 from the earliest stages of development causes the expression of another ion channel that can mediate DISC but does not normally do so. Therefore, to further test the hypothesis that TRPM4 is required for DISC, we constructed an shRNA directed against a unique sequence in the mouse TRPM4 gene and packaged it in the lentiviral vector FUGW, which also drives expression of the fluorescent marker EGFP. To test the efficacy of knockdown with the FUGW-shTRPM4 virus, we infected neural progenitor cells, which express endogenous TRPM4, and performed a Western blot using rabbit TRPM4 polyclonal antiserum (Fig. 7). Densitometric analysis of the TRPM4 band revealed that FUGW-shTRPM4 treatment reduced TRPM4 protein levels to 20% of those in uninfected cells. Treatment with empty FUGW yielded levels that were 96% of uninfected cells. Finally, treatment with FUGW engineering to express a nonsilencing shRNA yields TRPM4 protein levels that were 113% of uninfected cells.

Lentivirus-containing solutions were injected into the posterior cerebellar vermis of anesthetized juvenile mice using stereotaxic methods, and 1 wk was allowed for recovery and transduction. Slices of cerebellar tissue were prepared, and whole cell patch-clamp recordings were made from EGFP-positive Purkinje cells. Purkinje cells treated with the FUGW empty virus or the FUGW-nonsilencing shRNA virus expressed DISC with charge transfer of 0.57 ± 0.09 nC ($n = 18$) and 0.56 ± 0.1 nC ($n = 24$), respectively, which was not significantly different from each other. By contrast, treatment with FUGW-shTRPM4 produced a mean DISC charge transfer of 0.21 ± 0.06 nC ($n = 31$), a reduction to 37 ± 1% of the FUGW alone control values ($P < 0.01$). Control electrophysiological parameters such as membrane input resistance (R_{input}), whole cell capacitance (C_m, a measure of plasma membrane surface area, and thus cell size), and holding current (I_{hold}) did not differ significantly among FUGW alone, FUGW-nonsilence control, and the FUGW-shTRPM4 Purkinje cells. Thus shRNA-mediated knockdown of TRMPM4 produced a partial attenuation of DISC (~37% of control) that was similar to that observed in the TRPM4 null (~46% of control) or TRPM4/TRPM5 double null Purkinje cells (~35% of control).

DISCUSSION

The main finding of these experiments is that the DISC conductance has many hallmarks of TRPM4 and TRPM5 channels, being Ca-triggered, strongly permeant to Na and K but weakly Ca permeant, and strongly attenuated by a series of nonspecific TRPM4/5 blockers. Yet, it was only partially blocked by TRPM4 deletion, TRPM4 knockdown, or TRPM4/

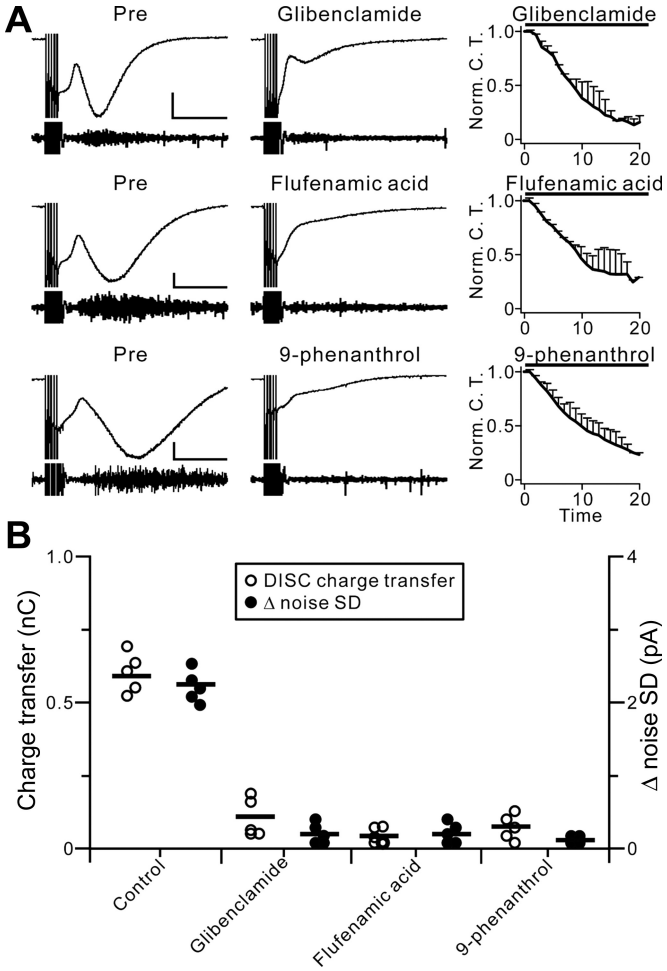

Fig. 4. Nonspecific TRPM4/5 channel blockers produce a near-complete attenuation of DISC. *A*: TRPM4/5 blockers were bath applied. All blockers produced a strong attenuation of DISC and the DISC-associated noise envelope. Representative DISC current and noise envelope traces are shown immediately before and 20 min after drug application. *Right*: time course of mean normalized DISC charge transfer. Scale bar: 200 pA, 2 s for DISC current trace and 19.6 pA, 2 s for noise envelope. *B*: population analysis of TRPM4/5 blockers. The DISC charge transfer and Δ noise SD are plotted. Each plot point represents a single cell after 20 min of drug exposure and the means are indicated by the horizontal bar. WT, wild type. $n = 5$ cells for untreated control, $n = 5$ cells for glibenclamide, $n = 5$ cells for flufenamic acid, and $n = 5$ cells for 9-phenanthrol.

TRPM5 double deletion. The observation that ~35–46% of DISC remained with these treatments indicates that, while TRPM4 may have some role in the DISC conductance, neither it nor TRPM5 are absolutely required.

Ca imaging experiments showed that DISC triggering, but not expression, was associated with a large Ca transient (Fig. 1). When combined with the low Ca permeability of the DISC conductance (Fig. 1), the observation that DISC was near-completely and reversibly blocked by substitution of external Na with the impermeant cation NMDG (Fig. 2) indicated that the DISC conductance was predominantly carried by Na influx. It is likely that K efflux also underlies this current but this was not tested here.

Previous work from our group had shown that DISC is weak in lobule VI of the cerebellar vermis but strong in more posterior regions such as lobule IX (Kim et al. 2009). Thus immunohistochemical experiments performed using slices of cerebellar vermis were encouraging when they showed TRPM4 and TRPM5 immunoreactivity in Purkinje cells of lobule IX but not VI (Fig. 3) as were results showing strong attenuation of DISC by three different nonspecific TRPM4/TRPM5 blockers, glibenclamide, flufenamic acid, and 9-phenanthrol (Fig. 4). As no specific blockers of TRPM4 and TRPM5 are presently available, we obtained null mice to test the hypothesis that these ion channels underlie DISC. While TRPM4 null Purkinje cells showed a significant but partial attenuation of DISC, DISC measured in TRPM5 null Purkinje cells was not significantly different from age-matched wild-type littermates. Double null Purkinje cells also showed partially attenuated DISC (Fig. 5). The attenuation of DISC in TRPM4 and TRPM4/5 DKO Purkinje cells is not likely to result from a side-effect on depolarization-evoked Ca transients as these were not significantly reduced (Fig. 6). Wild-type Purkinje cells transfected with a lentivirus engineered for shRNA-mediated knockdown of TRPM4 also showed partial attenuation of DISC (Fig. 7) consistent with the effect of TRPM4 deletion. Thus we believe

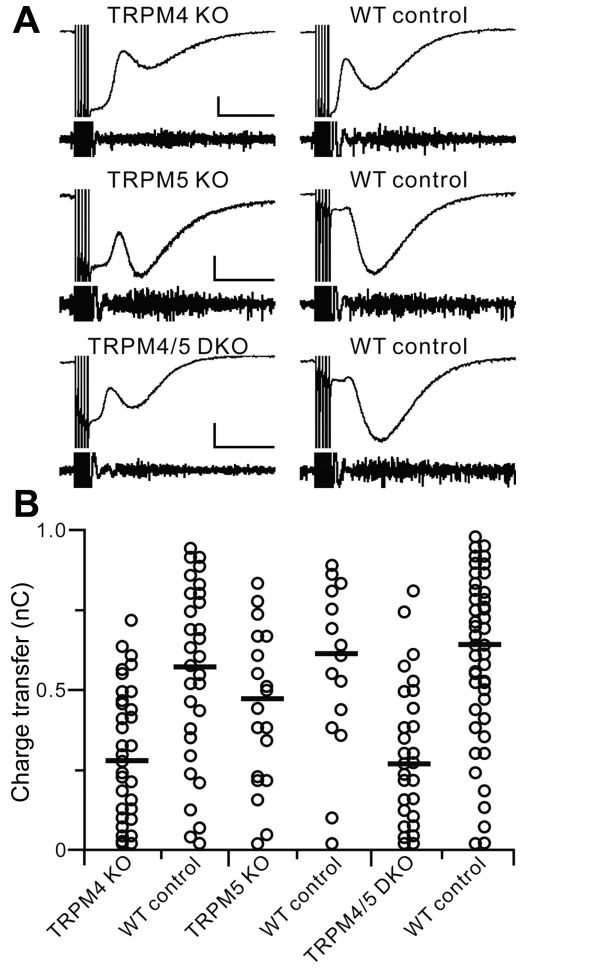

Fig. 5. DISC is partially attenuated in TRPM4 and TRPM4/5 double null Purkinje cells. *A*: because each mouse strain has a different genetic background, each was compared with its own age-matched wild-type littermate group. Representative DISC current and noise envelope traces are shown. Scale bar: 200 pA, 2 s for DISC current trace and 26 pA, 2 s for noise envelope. *B*: population analysis of TRPM4, TRPM5, and TRPM4/5 nulls. Each plot point represents a single cell and the means are indicated by the horizontal bars. $n = 40$ cells for TRPM4, $n = 31$ for its wild-type control; $n = 19$ cells for TRPM5, $n = 15$ for its wild-type control; $n = 28$ cells for TRPM4/5 DKO, $n = 46$ for its wild-type control.

that TRPM4 contributes to the DISC conductance but that neither it nor TRPM5 are absolutely required.

DISC was attenuated by the mGluR1 antagonist CPCCOEt, both in our hands (Shin et al. 2008) and in those of another group (Duguid et al. 2007). DISC was not blocked by either the NMDA receptor antagonist CPP or the AMPA/kainate receptor antagonist NBQX (Shin et al. 2008). This led us to suggest that the glutamate released from Purkinje cells by strong depolarization could also act in an autocrine fashion on mGluR1 to evoke DISC, mediated by previously described mGluR1-operated TRPC channels (Kim et al. 2003; Hartmann et al. 2008). However, further work in our group has invalidated this model (Shin et al. 2009). CPCCOEt, but not three other specific mGluR1 antagonists (JNJ16259685, 3-MATIDA, and Bay 36-7620), blocked DISC. This occurred even though all of these drugs produced near-complete blockade of inward currents evoked by application of the mGluR1/5 agonist DHPG. Most importantly, DISC was present in Purkinje cells derived from mGluR1 KO mice and mGluR1/mGluR5 DKO mice.

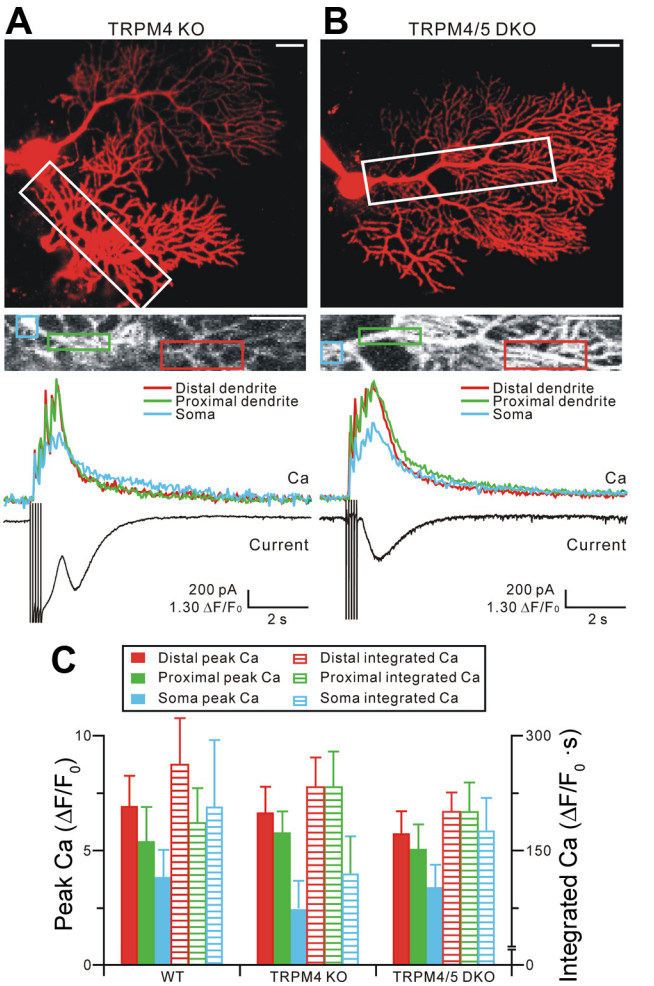

Fig. 6. Depolarization-evoked Ca transients are not attenuated in TRPM4 and TRPM4/5 double null Purkinje cells. *A*, *top*: projection of z series confocal images of a TRPM4 KO Purkinje cell filled with Alexa Fluor 594 and the attached patch pipette. *A*, *middle*: peak Fluo-5F Ca signal in a region of interest indicated by white box at *top*. Blue green and red boxes indicate subregions of interest used for Ca transient measurement in soma, proximal dendrite and distal dendrite, respectively. Scale bars: 20 μm for both *top* and *middle*. *A*, *bottom*: single, unaveraged simultaneously recorded Ca and DISC current traces from a representative Purkinje cell. *B*: same measurements described in *A* are applied to a Purkinje cell from a TRPM4/5 DKO mouse. *C*: population analysis of Ca transients in subregions of Purkinje cells. $n = 5$ cells/group.

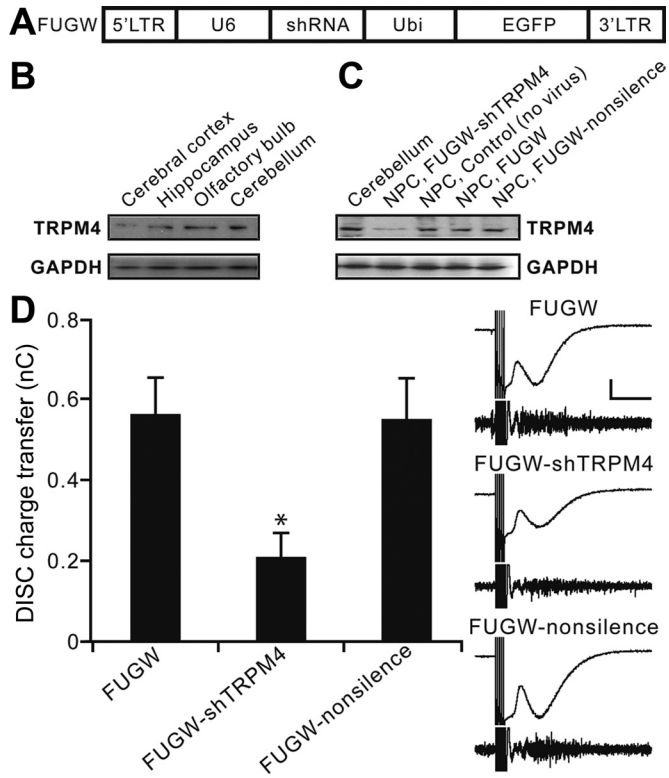

Fig. 7. Short hairpin (sh)RNA directed against the mouseTRPM4 channel produces attenuation of DISC. *A*: diagram of the bicistronic lentiviral vector (FUGW) used for in vivo genetic manipulation. *B*: TRPM4 expression levels are shown in various brain regions extracted from P17 mouse brain by Western blot analysis using polyclonal rabbit TRPM4 antibody directed against human TRPM4. *C*: in vitro validation of the efficacy of shRNA directed against the mouse TRPM4 gene. Adult neural progenitor cells (NPC) were infected with lentiviral constructs expressing shRNA directed against a unique sequence in mouse TRPM4. shRNA-TRPM4 (NPC, FUGW-shTRPM4), control (NPC, no virus), empty vector (NPC, FUGW), and nonsilence shRNA (NPC, FUGW-nonsilence) were tested. Equal amounts of cell lysate samples were subjected to western blot analysis. *D*: population analysis of the shRNA-TRPM4 knockdown effect on DISC amplitude. shRNA-TRPM4-containing lentivirus or control lentivirus was injected into the posterior cerebellar vermis of anesthetized juvenile mice using stereotaxic methods. About 1 wk later, cerebellar slices were prepared and DISC was recorded from EGFP-positive Purkinje cells derived from lentivirus transduced mice. The mean DISC charge transfer recorded from FUGW alone ($n = 18$), FUGW-shTRPM4 ($n = 31$), and FUGW-nonsilence ($n = 24$) conditions are plotted. Representative single, unaveraged DISC traces are shown. Scale bar: 200 pA, 2 s for DISC current trace and 23.8 pA, 2 s for noise envelope. *$P < 0.01$ by Mann-Whitney *U*-test for DISC charge transfer comparing FUGW-shTRPM4 to FUGW-nonsilence or FUGW-shTRPM4 to FUGW.

Recently, it has been shown that muscarinic receptor-modulated slow afterdepolarization in layer 5 pyramidal neurons of the medial prefrontal cortex shows a similar, partial attenuation in brain slices derived from TRPM4/TRPM5 DKO mice (Lei YT, Launay P, Margolskee R, Kandel ER, Siegelbaum SA, Thuault SJ, unpublished observations). Thus TRPM4 and TRPM5 may play similar roles in mediating slow, Ca-triggered conductances in different neuronal types.

ACKNOWLEDGMENTS

We thank Devorah Vanness for technical assistance, Richard Huganir for providing FUGW lentiviral vector and lentivirus, Robert Margolskee for

TRPM5 antibody, and members of the Linden and Song laboratories for helpful comments and discussion. Y. S. Kim especially thanks Eugene Kim from his heart.

GRANTS

This work was supported by National Institutes of Health Grants MH-51106 and MH-084020 (to D. J. Linden) and NS-047344 and AG-024984 (H. J. Song).

DISCLOSURES

No conflicts of interest, financial or otherwise, are declared by the author(s).

AUTHOR CONTRIBUTIONS

Author contributions: Y.S.K., J.H.S., H.S., P.L., and D.J.L. conception and design of research; Y.S.K., E.K., Y.M., and S.P. performed experiments; Y.S.K., E.K., Y.M., and S.P. analyzed data; Y.S.K., E.K., Y.M., S.P., and D.J.L. interpreted results of experiments; Y.S.K. prepared figures; Y.S.K. and D.J.L. drafted manuscript; Y.S.K., J.H.S., H.S., P.L., and D.J.L. edited and revised manuscript; Y.S.K., E.K., Y.M., S.P., J.H.S., H.S., P.L., and D.J.L. approved final version of manuscript.

REFERENCES

Ashcroft FM, Gribble FM. ATP-sensitive K^+ channels and insulin secretion: their role in health and disease. *Diabetologia* 42; 903–919, 1999.

Barbet G, Demion M, Moura IC, Serafini N, Léger T, Vrtovsnik F, Monteiro RC, Guinamard R, Kinet JP, Launay. The calcium-activated nonselective cation channel TRPM4 is essential for the migration but not the maturation of dendritic cells. *Nat Immunol* 9: 1148–1156, 2008.

Burnashev N, Villarroel A, Sakmann B. Dimensions and ion selectivity of recombinant AMPA and kainate receptor channels and their dependence on Q/R site residues. *J Physiol* 496: 165–173, 1996.

Crepel F, Galante M, Habbas S, McLean H, Daniel H. Role of the vesicular transporter VGLUT3 in retrograde release of glutamate by cerebellar Purkinje cells. *J Neurophysiol* 105: 1023–1032, 2011.

Damak S, Rong M, Yasumatsu K, Kokrashvili Z, Pérez CA, Shigemura N, Yoshida R, Mosinger B Jr, Glendinning JI, Ninomiya Y, Margolskee RF. Trpm5 null mice respond to bitter, sweet, and umami compounds. *Chem Senses* 31: 253–264, 2006.

Demion M, Bois P, Launay P, Guinamard R. TRPM4, a Ca^{2+}-activated nonselective cation channel in mouse sino-atrial node cells. *Cardiovasc Res* 73: 531–538, 2007.

Duan X, Chang JH, Ge S, Faulkner RL, Kim JY, Kitabatake Y, Liu XB, Yang CH, Jordan JD, Ma DK, Liu CY, Ganesan S, Cheng HJ, Ming GL, Lu B, Song H. Disrupted-In-Schizophrenia 1 regulates integration of newly generated neurons in the adult brain. *Cell* 130: 1146–1158, 2007.

Duguid IC, Pankratov Y, Moss GW, Smart TG. Somatodendritic release of glutamate regulates synaptic inhibition in cerebellar Purkinje cells via autocrine mGluR1 activation. *J Neurosci* 27: 12464–12474, 2007.

Earley S, Straub SV, Brayden JE. Protein kinase C regulates vascular myogenic tone through activation of TRPM4. *Am J Physiol Heart Circ Physiol* 292: H2613–H2622, 2007.

Fonfria E, Murdock PR, Cusdin FS, Benham CD, Kelsell RE, McNulty S. Tissue distribution profiles of the human TRPM cation channel family. *J Recept Signal Transduct Res* 26: 159–178, 2006.

Gardam KE, Geiger JE, Hickey CM, Hung AY, Magoski NS. Flufenamic acid affects multiple currents and causes intracellular Ca^{2+} release in Aplysia bag cell neurons. *J Neurophysiol* 100: 38–49, 2008.

Grand T, Demion M, Norez C, Mettey Y, Launay P, Becq F, Bois P, Guinamard R. 9-Phenanthrol inhibits human TRPM4 but not TRPM5 cationic channels. *Br J Pharmacol* 153: 1697–1705, 2008.

Guinamard R, Salle L, Simard C. The nonselective monovalent cationic channels TRPM4 and TRPM5. *Adv Exp Med Biol* 704: 147–171, 2011.

Guinamard R, Demion M, Magaud C, Potreau D, Bois P. Functional expression of the TRPM4 cationic current in ventricular cardiomyocytes from spontaneously hypertensive rats. *Hypertension* 48: 587–594, 2006.

Hartmann J, Dragicevic E, Adelsberger H, Henning HA, Sumser M, Abramowitz J, Blum R, Dietrich A, Freichel M, Flockerzi V, Birnbaumer L, Konnerth A. TRPC3 channels are required for synaptic transmission and motor coordination. *Neuron* 59: 392–398, 2008.

Hofmann T, Chubanov V, Gudermann T, Montell C. TRPM5 is a voltage-modulated and Ca(2+)-activated monovalent selective cation channel. *Curr Biol* 13: 1153–1158, 2003.

Kim YS, Shin JH, Hall FS, Linden DJ. Dopamine signaling is required for depolarization-induced slow current in cerebellar Purkinje cells. *J Neurosci* 29: 8530–8538, 2009.

Kim SJ, Kim YS, Yuan JP, Petralia RS, Worley PF, Linden DJ. Activation of the TRPC1 cation channel by metabotropic glutamate receptor mGluR1. *Nature* 426: 285–291, 2003.

Launay P, Fleig A, Perraud AL, Scharenberg AM, Penner R, Kinet JP. TRPM4 is a Ca^{2+}-activated nonselective cation channel mediating cell membrane depolarization. *Cell* 109: 397–407, 2002.

Launay P, Cheng H, Srivatsan S, Penner R, Fleig A, Kinet JP. TRPM4 regulates calcium oscillations after T cell activation. *Science* 306: 1374–1377, 2004.

Llano I, Leresche N, Marty A. Calcium entry increases the sensitivity of cerebellar Purkinje cells to applied GABA and decreases inhibitory synaptic currents. *Neuron* 6: 565–574, 1991.

Lois C, Hong EJ, Pease S, Brown EJ, Baltimore D. Germline transmission and tissue-specific expression of transgenes delivered by lentiviral vectors. *Science* 295: 868–872, 2002.

Ma DK, Jang MH, Guo JU, Kitabatake Y, Chang ML, Pow-Anpongkul N, Flavell RA, Lu B, Ming GL, Song H. Neuronal activity-induced Gadd45b promotes epigenetic DNA demethylation and adult neurogenesis. *Science* 323: 1074–1077, 2009.

Mrejeru A, Wei A, Ramirez JM. Calcium-activated non-selective cation currents are involved in generation of tonic and bursting activity in dopamine neurons of the substantia nigra pars compacta. *J Physiol* 589: 2497–514, 2011.

Nilius B, Mahieu F, Prenen J, Janssens A, Owsianik G, Vennekens R, Voets T. The Ca^{2+}-activated cation channel TRPM4 is regulated by phosphatidylinositol 4,5-biphosphate. *EMBO J* 25: 467–478, 2006.

Pompermayer K, Amaral FA, Fagundes CT, Vieira AT, Cunha FQ, Teixeira MM, Souza DG. Effects of the treatment with glibenclamide, an ATP-sensitive potassium channel blocker, on intestinal ischemia and reperfusion injury. *Eur J Pharmacol* 556: 215–222, 2007.

Riera CE, Vogel H, Simon SA, Damak S, le Coutre J. Sensory attributes of complex tasting divalent salts are mediated by TRPM5 and TRPV1 channels. *J Neurosci* 29: 2654–2662, 2009.

Sabovcik R, Li J, Kucera P, Prod'hom B. Permeation properties of a Ca(2+)-blockable monovalent cation channel in the ectoderm of the chick embryo: pore size and multioccupancy probed with organic cations and Ca2+. *J Gen Physiol* 106: 149–174, 1995.

Shin JH, Kim YS, Worley PF, Linden DJ. Depolarization-induced slow current in cerebellar Purkinje cells does not require metabotropic glutamate receptor 1. *Neuroscience* 162: 688–693, 2009.

Shin JH, Kim YS, Linden DJ. Dendritic glutamate release produces autocrine activation of mGluR1 in cerebellar Purkinje cells. *Proc Natl Acad Sci USA* 105: 746–750, 2008.

Takahira M, Sakurai M, Sakurada N, Sugiyama K. Fenamates and diltiazem modulate lipid-sensitive mechano-gated 2P domain K(+) channels. *Pflügers Arch* 451: 474–478, 2005.

Ullrich ND, Voets T, Prenen J, Vennekens R, Talavera K, Droogmans G, Nilius B. Comparison of functional properties of the Ca^{2+}-activated cation channels TRPM4 and TRPM5 from mice. *Cell Calcium* 37: 267–278, 2005.

Vennekens R, Nilius B. Insights into TRPM4 function, regulation and physiological role. *Handb Exp Pharmacol*, 269–285, 2007.

Zhang Y, Hoon MA, Chandrashekar J, Mueller KL, Cook B, Wu D, Zuker CS, Ryba NJ. Coding of sweet, bitter, and umami tastes: different receptor cells sharing similar signaling pathways. *Cell* 112: 293–301, 2003.